

<https://doi.org/10.1038/s42003-025-08125-5>

# Decoupled respiration in electro-active bacteria

Check for updates

Diego A. Massazza , Juan P. Busalmen &amp; Hernán E. Romeo

Studies on electron-transfer pathways in certain bacterial strains have revealed that the degree of coupling of electron transfer to proton translocation along the respiratory chain can be regulated according to metabolic demands. This first line of metabolic response, based on the existence of energy dissipation mechanisms, has not been demonstrated to be a general pattern across the bacterial kingdom, let alone to be operative in electro-active bacteria. In this study, we hypothesized that electro-active cells should respond to over-polarization by also triggering energy decoupling mechanisms to prevent metabolic overloads. Based on electrochemical analyses, we propose that the recently discovered inner-membrane cytochrome CbcBA - used by electro-active *Geobacter sulfurreducens* bacteria for cellular respiration near the thermodynamic energetic limit - can also act as an energy dissipation gate when the metabolism is demanded, contributing to regulate the energy balance of the cell by decoupling carbon assimilation from electrode respiration.

Living organisms are open thermodynamic systems that exchange matter and energy with the environment<sup>1</sup>. At cellular level, life depends on the regular external supply of electron/carbon sources to get a significant driving force to maintain the living system out of equilibrium (steady state)<sup>2</sup>. Microbial existence is a typical and well-known example of unicellular life where the structural and functional order arises under non-equilibrium conditions; however, due to the complexity of cell functioning, the metabolic mechanisms behind energy management control are not fully understood yet.

Electron-transfer reactions play a fundamental role in biological respiration and energy conservation processes, taking place between molecular components in a chain of thermodynamically and kinetically favorable events used to generate transmembrane proton gradients, which in turn lead to the establishment of a proton motive force (*pmf*) that the cell uses to synthesize ATP as the primary form of conserved energy<sup>3</sup>. However, this is the case only if the catabolic energy-producing path is efficiently coupled to the energy storage process. Studies on electron-transfer pathways in certain bacterial strains indicate that the degree of coupling of electron transfer to proton translocation can be finely tuned by the microbial machinery according to metabolic demands, this occurring regardless of the thermodynamic hierarchy of the electron gates involved along the respiratory chain<sup>4,5</sup>. This mechanism seems to have been designed so as to function as a metabolic drain, through which the microorganisms can free themselves from all of the excess internal entropy they cannot help producing as a consequence of the irreversible metabolic activities. This gives rise to energy dissipation in the form of heat and/or chemical entropy<sup>6</sup>, due

to an incomplete energy coupling between the catabolic process and the ATP synthesis. This first line of metabolic response, that seems to regulate the energy balance in some microbial strains, has not been demonstrated to be a general pattern across the bacterial kingdom, let alone to be operative in electro-active bacteria, the latter being capable of coupling intracellular organic matter oxidation with extracellular reduction processes<sup>7</sup>. Due to the fact that dissipation mechanisms play a central role in the metabolism of all living forms, and building on the existence of an upper limit on Gibbs energy dissipation for sustaining life<sup>8</sup>, we hypothesized that electro-active bacteria should respond to external polarization beyond that supporting maximal energy production by also triggering decoupling mechanisms, so as to prevent metabolic overloads induced by this non-natural condition.

In this study, to experimentally test our hypothesis, we electro-chemically grew electro-active *G. sulfurreducens* biofilms at increasing polarization potentials to study their voltammetric response, in the search for redox centers participating of the electron-transfer process out of the cell with the expectancy of finding clues leading to metabolic decoupling mechanisms. As a result, we here provide evidence on the recruitment of CbcBA - a recently discovered low-potential inner-membrane *bc*-type cytochrome in *G. sulfurreducens* that barely contributes to the generation of the *pmf*- as an electron-transfer path operating also at high potential beyond that which maximizes respiration, leading to a steep drop in cell energy conservation. This counteracting response, by using a low-potential electron gate when the cell is exposed to extreme oxidative conditions, contributes to regulate the metabolic energy balance of the electro-active cell, with CbcBA functioning as a decoupling gate.

Institute of Materials Science and Technology (INTEMA), University of Mar del Plata (Mar del Plata, Argentina) and National Research Council (CONICET, Argentina), Mar del Plata, Argentina. ✉e-mail: [dmassazza@fi.mdp.edu.ar](mailto:dmassazza@fi.mdp.edu.ar); [hromeo@fi.mdp.edu.ar](mailto:hromeo@fi.mdp.edu.ar)

## Results and discussion

### *G. sulfurreducens* inner-membrane cytochromes display performance flexibility as a function of the external potential

Studies on electron-transfer pathways in *G. sulfurreducens* have demonstrated that at least three different potential-dependent electron gateways - the inner-membrane cytochromes CbcBA, CbcL and ImcH - are functional in channeling electrons out of the cell<sup>9-11</sup>. In accordance with the effective midpoint potentials associated to the metabolic pathways involving each protein (around  $-0.21$  V vs SHE for CbcBA,  $-0.15$  V for CbcL, and  $-0.05$  V for ImcH)<sup>10,12,13</sup>, the latter are employed during respiration to harvest different amounts of free energy ( $\Delta G$ ) depending on the associated  $H^+/e^-$  stoichiometry. On this basis, we tested our hypothesis that electroactive microorganisms should count on dissipative mechanisms when taken to an overloaded respiration. To do this, we grew *G. sulfurreducens* biofilms on graphite electrodes polarized at different potentials ( $-0.23$  V;  $-0.15$  V;  $0$  V;  $+0.2$  V;  $+0.4$  V and  $+0.5$  V vs SHE), and performed cyclic voltammetry analyses once stationary growth was reached to confirm the occurrence of the typical S-shaped oxidative-catalysis process for all of the biofilms at all potentials (Supplementary Material, Supplementary Section SM-1, Supplementary Fig. SM-1).

The first derivatives of the obtained voltammograms indeed revealed the participation of the three cytochromes in generating the catalytic signal, but showed potential-dependent differences in their contribution to the overall current (Supplementary Material, Supplementary Section SM-2, Supplementary Fig. SM-2). To calculate the individual cytochrome participation to the total electron flux out of *G. sulfurreducens* we applied the three-site limiting current approach described by Zacharoff et al. and Howley et al.<sup>12,14</sup>. Our strategy here was focused on analyzing any differences arose in the voltammetry curves, evaluating the participation of each cytochrome as electron-transfer path out of the cell by fitting the entire voltammetry profile. The confirmation of the potential-dependent response by the shifting of the catalytic curve was taken as an indication of the influence of the growth conditions on the involved paths. The results are summarized in Fig. 1.

The gradual changes in contribution to the total current for each of the three cytochromes as the growth potential was varied were considered as a proxy of the polarization-dependent variations in the electron-transfer paths experienced during growth, suggesting somehow the branching of the electron flow out of the cell while growing under different polarization conditions. In agreement with previous studies<sup>10</sup>, our results indicate that CbcBA is used by *G. sulfurreducens* as the main electron gate when the cell faces energy limitations as a consequence of the low potential of the electron acceptor ( $-0.23$  V vs SHE), this leading to an energetic balance that is only enough to meet cellular maintenance requirements, a condition fulfilled when the *pmf* approaches zero. As the electrode potential is raised, and the total current reaches to the absolute maximum, the participation of CbcBA markedly drops to a minimum level of activity (which was sustained up to  $+0.4$  V) (Fig. 1), being replaced by the transporter associated to the second proton pump (CbcL), which takes the role of the main electron gate in the  $-0.15/+0.4$  potential window. The inverse correlation between the two low-potential proteins is complemented by a continuous increase of the activity of ImcH along the potential window (Fig. 1), the third coupling site in the transport chain. Set in a thermodynamic frame, in which the inner-membrane cytochromes are organized in a redox sequence that would allow the efficient switching from low- to high-potential electron-transfer pathways as the external potential is raised, the electrochemical activity detected here for the three cytochromes as a function of the electrode potential deserves a first comment. Whereas a mechanism through which the activation of a high-potential gate would be coupled to the shutting off of the preceding lower-potential path is consistent with experimental evidence collected on single/multiple mutant strains (deletions of genes encoding CbcBA, CbcL or ImcH), the underlying potential/electron-gate mechanism in wild-type (WT) strains could a priori pose a different scenario, leading to a non-identical behavior compared to that of mutant microorganisms<sup>15</sup>. Although the electrochemical activity of ImcH as an electron gate could

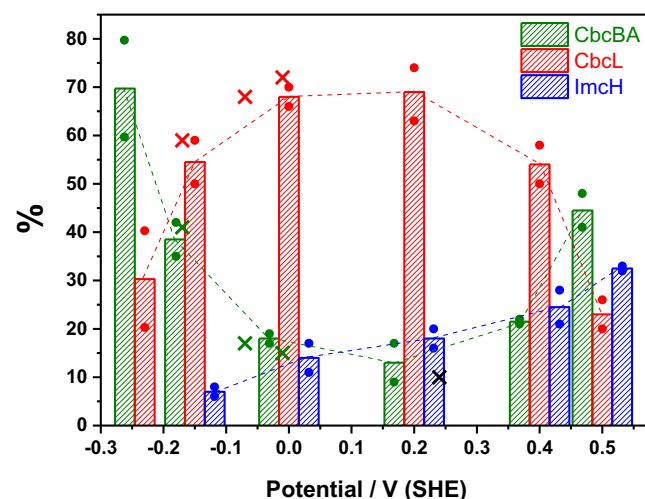


**Fig. 1 | Electron-transfer path splitting along the inner-membrane of *G. sulfurreducens* as a function of the external electrode potential.** The three cytochromes are active regardless of the external potential at which the biofilms were grown (except for the lowest potential tested, at which only CbcBA and CbcL were detected), thus partitioning the catabolic energy along the inner membrane. The electron path splitting through each cytochrome (represented as % of participation) depends on both the amount of each cytochrome along the electron-transport chain (given by genetic control) and their biochemical activity (metabolic control). For comparative purposes, the results are displayed together with those reported in previous studies: red crosses (CbcL activity)<sup>14</sup>, green crosses (CbcBA activity)<sup>14</sup>, black cross (CbcBA activity)<sup>16</sup>.  $n = 2$  (independent experiments for each potential tested, represented as dots).

have been anticipated to take center stage as the electrode potential was raised, the obtained results are not unexpected, lining with previous studies that have already revealed a higher participation of CbcL (compared to that of ImcH) at potentials at which a higher involvement of ImcH would have been beforehand awaited<sup>14</sup>. Additional support to the activity not only of CbcL, but also of CbcBA, above  $-0.1$  V was reported by Marsili et al.<sup>16</sup>. In line with these studies, Zacharoff et al. demonstrated that in fact CbcL contributes to over 60% of the total current at  $+0.24$  V in WT strains<sup>12</sup>, in excellent agreement with the results depicted in Fig. 1. In this scenario, and according to current literature on metabolic gradients identified throughout biofilms as they approach the stationary state under continuous cultures, we should also be cautious and point initially on the possibility that not all the cells along the biofilm would be experiencing the same effective potential, which could also contribute to the observed potential-dependent effect. This point will be further addressed in sections below.

Taking into consideration that the electron flow through each of the three inner-membrane cytochromes is thermodynamically (and kinetically) feasible - added to the fact that electro-active bacteria rely on branched respiratory chains associated to multiple metabolic electron-flux patterns - it would not be surprising that in WT strains the three electron gateways might take part simultaneously (although in different proportions) of the electron-transfer process in a range of external potentials. In the present study we intend to contribute to the current knowledge on the electrochemical behavior of the inner-membrane cytochromes in *G. sulfurreducens*, demonstrating their dynamic flexibility as a function of the electrode potential. As to this flexibility, when the potential was poised beyond that supporting maximum current generation ( $+0.4$  V), an unexpected contribution of the lowest-potential CbcBA cytochrome was noticeably detected (Fig. 1,  $+0.5$  V), working together with the other two paths, but becoming the main route for transferring electrons out of the cell. In accordance with the above mentioned, two scenarios initially arise: (i) or CbcBA takes a center role in far-from-the-electrode bacteria exposed to lower effective potentials, under a condition in which the bacteria near the electrode would be prevented from functioning at full metabolism maybe

caused by local stress at high potential (+0.5 V); or (ii) as it bypasses the thermodynamic hierarchy of the electron transporters, the result obtained would be a consequence of a mechanism of proton pump (energy) regulation along the inner-membrane, compatible with the existence of an overall physiological flexibility.

The respiratory flexibility proposed here for *G. sulfurreducens* is not unknown in cellular dynamics, representing a strategy used not only by bacteria (like *E. coli* and/or *P. pantotrophus*)<sup>4,5</sup>, but also by eukaryotes through modulation of the activity of the complexes I, III and IV along the mitochondrial respiratory chain<sup>17–19</sup>. This mechanism supports electron-transfer regulation through inner-membrane proteins (e.g., heterodimeric reductases, terminal oxidases) that display flexible activity to counteract extreme metabolic changes. In bacteria, respiration flexibility has been nicely demonstrated for example in *P. pantotrophus*, where the presence of nitrate reductases alongside multiple oxidases in the respiratory chain during the aerobic growth of the microorganism seems to respond to a tight metabolic control. In analogy to our results, *P. pantotrophus* up-regulates - strikingly under excess oxygen - an inner-membrane system (the NapABC complex) which catalyzes the reduction of nitrate without contributing to proton translocation<sup>20</sup>. This system is used as an electron gate that prevents the building-up of an excessive transmembrane proton gradient (acidification of the periplasm). Similarly, *E. coli* has also been demonstrated to exhibit strong respiratory flexibility, by decoupling catabolism from ATP synthesis through the use of an inner-membrane cytochrome (cytochrome *bd-II* oxidase) that plays the role of an electron carrier that does not contribute to the *pmf*<sup>4</sup>. Likewise, a number of studies have also reported on the dropping of the microbial growth yield when the metabolism is demanded, suggesting the existence of an active energy-wasting mechanism at the core of the microbial respiratory chain<sup>21,22</sup>. This leads to wide variation in microbial energetic efficiencies, as an adaptive response to changes in the electron influx into the respiratory chain and/or to the potential of the available electron acceptors<sup>23</sup>.

According to this background, we anticipated that the flexibility evidenced in the participation of the three inner-membrane cytochromes in *G. sulfurreducens* might play a central role in the energy partitioning mechanisms inside the electro-active cell. We then speculated that the proton translocation activity of each electron-transfer path might offer clues on possible dissipation gates. The two constitutively expressed cytochromes ImcH and CbcL have been demonstrated to effectively contribute to the *pmf* when operating as electron paths, although supporting different growth yields; with ImcH being essential for respiration under energy-plentiful conditions, a situation encountered when *G. sulfurreducens* faces high-potential acceptors and/or electrodes poised above  $-0.1$  V (SHE)<sup>13</sup>. As a complement, CbcL has been demonstrated to couple electron transfer to proton translocation when the redox potential falls below  $-0.1$  V<sup>24</sup>; whereas the recently discovered *bc*-type cytochrome CbcBA has been shown to be essential for respiration when the cell accesses only to limited energy, acting as a path that barely contributes to proton translocation<sup>10</sup>.

By considering the Gibbs energy change associated to the electron-transfer processes involved in proton translocation during respiration ( $\Delta G_{e^-}$ ), and regarding that the driving redox reaction is the only energy source feeding the translocation activity ( $\Delta G_{H^+}$ ), it is possible to estimate the maximum amount of protons that could be translocated per electron through each protein ( $H^+/e^-$  ratio) on the basis of upper limits imposed by energy conservation<sup>25,26</sup>. In stark contrast to linear electron-transport chains in eukaryotes, electro-active bacteria rely on branched respiratory chains associated to multiple metabolic electron-flux patterns. This poses certain difficulties when it comes to identifying the redox counterparts involved in proton translocation through CbcBA, CbcL and ImcH; especially when the electron-transfer out of the cell requires multiple soluble carriers (not yet univocally identified) across the periplasm. Recognizing that energy conservation takes place at the inner-membrane level, it is still possible to make an estimation of the maximum energy available to translocate charges along the respiratory chain of *G. sulfurreducens*. According to reported

physiological data, respiratory membranes for different strains and under a variety of conditions exhibit *pmf* values spanning 130–200 mV<sup>27–30</sup>. Due to the lack of experimental *pmf* data for *G. sulfurreducens*, we approached this value to the one experimentally measured for *E. coli* growing under anaerobic conditions (140 mV)<sup>27</sup>, on the basis of conserved structural and functional respiratory patterns across the bacterial domain<sup>31</sup>. Thus, an energy of 13.5 kJ would be required in *G. sulfurreducens* to translocate a minimum of one mol of charge against its electrochemical potential. By considering the maximum energy available along the inner membrane up to the location of each cytochrome, maximum  $H^+/e^-$  ratios of  $\sim 0.8$ , 1.2 and 1.9 would be accessible when CbcBA ( $\Delta G_{CbcBA} = -10.6 \frac{\text{kJ}}{\text{mol } e^-}$ ), CbcL ( $\Delta G_{CbcL} = -16.4 \frac{\text{kJ}}{\text{mol } e^-}$ ) and ImcH ( $\Delta G_{ImcH} = -26.0 \frac{\text{kJ}}{\text{mol } e^-}$ ) take part of the electron transfer process, respectively. These values only set upper limits given by energetic constraints, the physiological number of charges effectively translocated depending on the periplasmic redox counterparts for each cytochrome and the coupling efficiency of each gate, the latter finally dictated by external boundary conditions.

According to its thermodynamic hierarchy, and in agreement with recently published results<sup>10</sup>, CbcBA would be effectively involved in a path contributing to a much lesser extent to proton translocation compared to the other two inner-membrane cytochromes, marginally providing energy to translocate one proton per electron even at a hypothetical case of 100% coupling efficiency. Interestingly,  $H^+/e^-$  ratios lower than unity have been reported to be operative, for example, in the complex I of *E. coli* and other bacteria, when the Gibbs energy of the driving redox reaction is not enough to meet the corresponding proton translocation stoichiometry. In these cases, additional energy sources which partially dissipate the membrane electrochemical potential (e.g.,  $Na^+/H^+$  antiporter mechanisms) are needed to build up the remaining energy for net translocation according to the cell needs<sup>32,33</sup>. In this scenario, the results shown in Fig. 1 can be interpreted in the context of the existence of parallel electron routes out of *G. sulfurreducens* depending on the external conditions, with the three cytochromes playing a simultaneous active role and CbcBA acting as a metabolic way out far from equilibrium marginally contributing to the *pmf*.

Energy transduction mechanisms associated to coupled processes, like redox-coupled proton translocation phenomena, are typically addressed within the formalism of linear non-equilibrium thermodynamics, as long as the linearity of the flux-force functions of the coupled phenomena can be guaranteed<sup>19,34</sup>. This can only be ensured in regions about the equilibrium - at moderate growing conditions - where Onsager symmetry relations hold; however, at critical distances far from equilibrium the linear behavior cannot longer be assumed. In this sense, under a demanded metabolism - like the one induced under polarization at extreme external potentials - it would be in principle expected the charge-translocating energy converters to move from the linear regime, leading to  $H^+/e^-$  stoichiometries deviating even more from the maximum values dictated by the energetic upper limits. This probably represents a challenge for cell homeostasis in terms of, for example, local pH gradients, supporting the role of the molecular complex involved in the path of lowest  $H^+/e^-$  ratio (CbcBA) as an emergency gate.

In a scenario in which coupled linear processes cannot be ensured, and due to the lack of both mechanistic and molecular information on proton translocation activities for each cytochrome in *G. sulfurreducens*, the  $H^+/e^-$  stoichiometric description above was complemented with calculations of energy balances associated to the experimentally determined production of microbial biomass as a function of the imposed external potential.

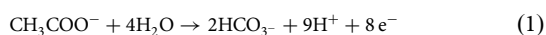
### CbcBA activation at high potentials lessens carbon assimilation

To further explore energetic balances in response to the potential of the electron acceptor, biomass yields were calculated on the basis of acetate consumption ( $Y_{X,Acetate}$ ). For this, experimental bacterial counting data were combined with the amount of electron/carbon donor consumed at each growing potential. The relation between the amount of acetate consumed and the corresponding biomass produced, the latter expressed as

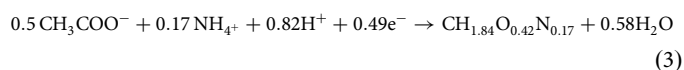
C-mol of *G. sulfurreducens*, was determined by identifying the catabolic and anabolic reactions involved in the production of *G. sulfurreducens* cells, establishing for this the macrochemical equation for the heterotrophic growth on acetate.

From a physicochemical point of view, and in stark contrast to isolated or closed systems, living organisms are open thermodynamic systems that exchange matter and energy with the environment. Chemotrophic life thus depends on the regular external supply of electron/carbon sources to get a significant driving force to maintain the living system in steady state. In this frame, to calculate the relation between the total amount of acetate consumed by *G. sulfurreducens* and the corresponding biomass produced, we first identified the catabolic and anabolic reactions that take place in the heterotrophic production of *G. sulfurreducens* cells growing on acetate. The microbial metabolism is typically simplified by considering the overall catabolic and anabolic reactions coupled by an energy carrier (ATP). The stoichiometry of these coupled reactions further allows to define mass, charge and Gibbs free energy balances, from which the biomass yield on the corresponding electron/carbon source can be finally determined<sup>2</sup>.

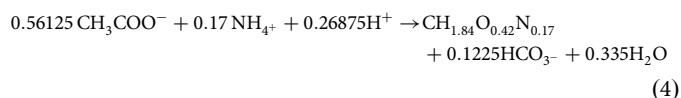
After being taken up by the cell, part of the acetate is oxidized in the catabolic reaction to produce energy, while the remaining is employed in the anabolic reaction to produce new cells. The catabolic reaction corresponding to the oxidation of acetate is (per mol of electron donor):



Acetate molecules not used in the catabolic reaction are diverted to the anabolic process. Electron transfer in the anabolism depends on the oxidation state of the carbon source compared to that of biomass. When the degree of reduction of the carbon source is lower than that of biomass, the substrate has to act not only as a source of carbon, but to the electrons as well. According to the degree of reduction of acetate (4 mol e<sup>-</sup>/C-mol acetate) and the elemental composition of one C-mol of *G. sulfurreducens* (CH<sub>1.84</sub>O<sub>0.42</sub>N<sub>0.17</sub>, 4.49 mol e<sup>-</sup>/C-mol *G. sulfurreducens* cell)<sup>35</sup>, part of the acetate diverted to the anabolic reaction is first oxidized to supply the electrons necessary to reach the degree of reduction of biomass, while the remaining is used as carbon source. These reactions can be represented as:



where the reaction (2) embodies the oxidation of acetate to supply the electrons needed in the production of one C-mol biomass (reaction (3)). According to (2) and (3), the overall anabolic reaction for the production of one C-mol of *G. sulfurreducens* is given by:



The stoichiometries of the reactions (1) and (4) were finally used to link the total amount of acetate consumed - both that consumed in the oxidation process (calculated from the electrical charge experimentally determined from the chronoamperometries once steady state was reached) plus that used in cell synthesis - and the C-mol of *G. sulfurreducens* cells grown (experimentally measured) for each of the conditions evaluated. The Table shown in the Supplementary Material (Supplementary Section SM-3) depicts the calculated biomass yields ( $Y_{X,\text{Acetate}}$ ) expressed as moles of carbon of biomass (C-mol) per mol acetate consumed. Figure 2 below shows the obtained biomass yields as a function of the electrode potential.

The biomass yield showed a positive exponential trend as a function of the external potential in the -0.23 V/+0.4 V window, increasing the biomass production per unit acetate consumed as the energy became

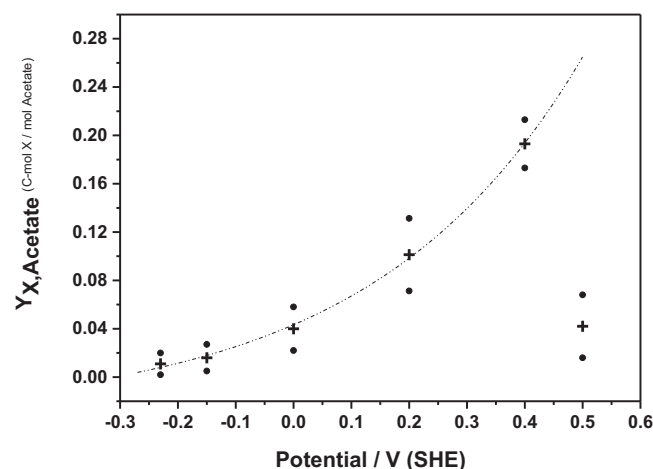


**Fig. 2 | *G. sulfurreducens* cell yield based on acetate oxidation as a function of the electrode potential.** Microbial yield revealed the effect of two opposing mechanisms: at low potentials (low available energy) proton translocation barely contributes to ATP synthesis; at extreme high potentials (demanded respiration) dissipating mechanisms lead to low carbon assimilation efficiencies.  $n = 2$  (independent experiments for each potential tested, represented as dots).

increasingly available. When the biofilm was grown at +0.5 V, the yield abruptly dropped to values well comparable to those for biofilms growing under limiting energy at the lowest potentials, indicating that most of the energy was not directed to growth. Analyzed in context with the increased contribution of CbcBA as the main electron-transfer path at +0.5 V (Fig. 1), the result is compatible with a considerable fraction of the available electrons flowing through a route of low proton translocation activity, thus not leading to significant biomass production. From an energetic point of view, this supports the occurrence of an energy dissipation mechanism to maintain cell viability. This is consistent with thermodynamic efficiency calculations ( $\eta$ , Supplementary Material, Supplementary Section SM-4, Supplementary Fig. SM-4), the latter representing the fraction of the catabolic energy that is effectively conserved in the anabolic reaction.

Interestingly, the thermodynamic efficiency calculated from the catabolic energy partitioning can in turn be linked to the overall thermodynamic efficiency of the energy converters along the respiratory chain; in particular, to the redox-driven proton translocation processes and the associated output/input powers (forces and fluxes) of the two coupled phenomena<sup>19</sup>:

$$\eta = -\frac{J_H \cdot pmf}{J_e \cdot \Delta E} \quad (5)$$

where  $J_H$  is the net proton flux,  $J_e$  the electron flux,  $pmf$  the proton motive force and  $\Delta E$  the corresponding redox span. The negative sign implies that the proton flux occurs uphill; that is, against its conjugate force ( $pmf$ ). Although relations of the form shown in Eq. (5) have been typically used for the description of linear energy converters<sup>19,34,36</sup>, the dissipation function from which energy efficiency correlations are derived is valid unrestrictedly, regardless the formalism is addressed in the Onsager region or not<sup>37</sup>. Thus - within the phenomenological description of the coupled energy transduction processes and their relation to the thermodynamic efficiency calculated - at maximum redox input, a lower thermodynamic efficiency can only indicate a lower net proton flux and/or  $pmf$ , or a higher electron flux. The recruitment at +0.5 V of the electron gate involved in the pathway of lowest H<sup>+</sup>/e<sup>-</sup> stoichiometry (CbcBA), along with a maximal overall electron flux out of the cell (1.78 pA/cell at +0.5 V compared to 0.46 pA/cell at +0.4 V, determined from bacterial counting and current density measurements at steady state), support the lower thermodynamic efficiency at the highest potential, in a scheme in which CbcBA acts as a dissipative path contributing to decouple the anabolic process from the electrode respiration.

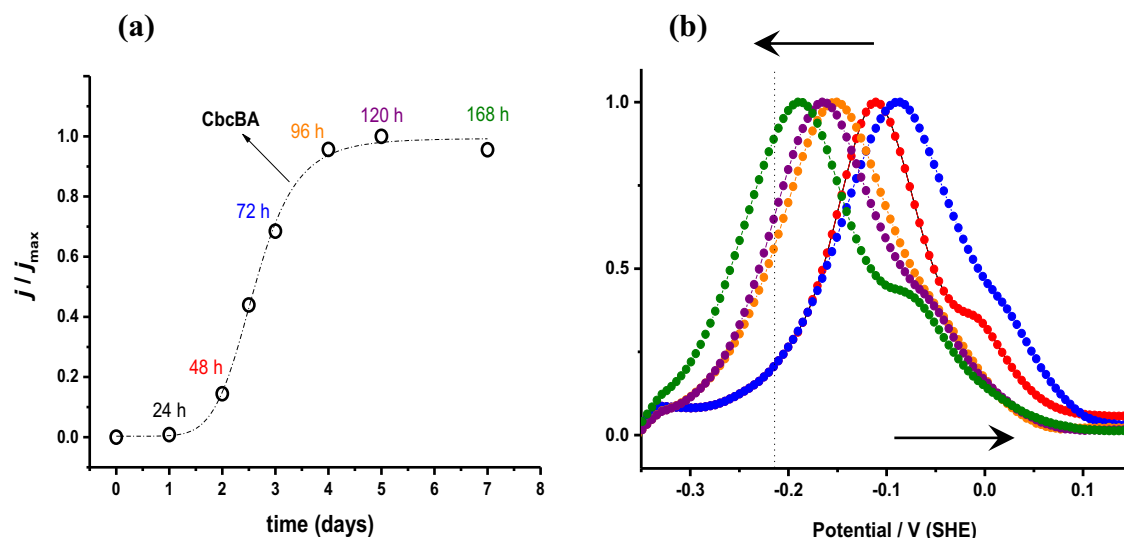


**Fig. 3 | Electrochemical behavior of the inner-membrane cytochromes in *G. sulfurreducens* as a function of biofilm evolution at +0.5 V (SHE). a** Normalized chronoamperometry under catalytic conditions; **b** first derivatives of the voltammograms collected at different growing stages along the chronoamperometry evolution. The broken line in (b) indicates the mid-point potential associated to the

metabolic path involving mainly the participation of CbcBA. Colors are related in each figure to a particular growing stage. A progressive shift to higher potentials was evidenced in the first 72 h (right-pointing arrow in (b)), reversing back to lower potentials as CbcBA takes over (left-pointing arrow).

In essence, as the potential exceeds that which maximizes respiration (+0.4 V), an increased portion of the energy derived from the catabolic reaction is wasted, requiring metabolic decoupling mechanisms for this to occur. The recruitment of the lowest-midpoint potential inner-membrane cytochrome CbcBA, matching the point at which the cells were taken to an overloaded respiration, reveals the response of the electro-active cells against the pressure exerted by a metabolism pushed to the limit.

In this context it is important to highlight that the energy balance, together with voltammetry results (addressed in the next section), indicates that the CbcBA activity at the highest potential cannot be attributed to a distance-dependent drop in redox potential along the biofilm. If that were the case, the higher bacterial counting measured for the biofilm grown at +0.4 V ( $1.39 \times 10^7$  bacteria  $\text{cm}^{-2}$ ) should have displayed a concomitant higher participation of CbcBA compared to that at +0.5 V ( $3.94 \times 10^8$  bacteria  $\text{cm}^{-2}$ ), rather than the opposite trend (Fig. 1). In order to rule out possible drops in biomass counting due to cell detachment associated to harmful conditions (in the event they had occurred, triggered by the high potential), planktonic cell counts were also performed in the reactor media. The results showed that - both at +0.4 and +0.5 V - around 90% of the total biomass was present in the biofilms. Revisiting the literature on the area, our results were pretty much the same as those previously reported for *G. sulfurreducens*<sup>38</sup>, demonstrating similar biofilm dynamics regardless of the external potential. This fact gives additional support to the sudden drop in cell replication on the electrode surface as a consequence of the activation of CbcBA at the highest potential tested.

Out of the relevant practical consequences that the presented results could have in the area of bio-electrochemical current generation it is to be highlighted that, although there were noticeable differences in biomass production, the electrical current density reached by the biofilms grown at +0.4 V and +0.5 V was well comparable (Supplementary Material, Section SM-5, Supplementary Fig. SM-5). This would bring about a profound impact on power-generating bio-electrochemical systems, counting on active cells working at their most while avoiding at the same time futile biomass accumulation occurring in typical physiological stratification events that lead to the drop of the mean electrochemical performance<sup>39</sup>. In other words, polarization beyond that required for maximal current production may prevent accumulation of cells that do not contribute to current production, thus leading to an optimized technological performance.

### CbcBA is recruited in the late exponential/early stationary phase at +0.5 V (SHE)

It is known that both *cbcl* and *imcH* are constitutively expressed in *G. sulfurreducens*; however, unlike its inner-membrane partners, *cbcBA* transcription is metabolically regulated, requiring the  $\sigma^{54}$ -dependent BccR regulator to be expressed<sup>10</sup>. To gain insight into the recruitment of CbcBA over time during the evolution of the microbial biofilm grown at +0.5 V, cyclic voltammetry scans were performed at different growing stages along the chronoamperometry evaluation. Figure 3 shows the chronoamperometry of the biofilm at +0.5 V, along with the first derivatives of the voltammograms collected at different evolution times.

No catalytic signals of CbcBA were detected during the first days of evolution (up to 72 h, included), indicating that neither the early biofilm nor the exponentially-growing microorganisms seem to have needed this cytochrome to channel electrons out of the cell along the first growing phase. This, as expected, agrees with the non-constitutive nature of CbcBA. However, a strong shift of the midpoint towards lower potentials - matching the slowing down of growth - was clearly observed in the late exponential/early stationary phase (beyond 72 h), continuously evolving and becoming more negative well into the stable stationary phase (168 h). This result is in sharp agreement with those reported by Joshi et al.<sup>10</sup>, who demonstrated that the expression of the *cbcBA* operon in *G. sulfurreducens* growing on Fe(III)-citrate is strongly up-regulated at the late exponential/early stationary stage, but not before.

The results shown in Fig. 3b reveal overall physiological shifts during the biofilm evolution, calling again the attention to the causes triggering CbcBA appearance. As mentioned along the discussion of the results shown in Fig. 1, CbcBA could take part of the electron transfer process at extreme potentials as a consequence of a potential drop along the developing biofilm (with far-from-the-electrode bacteria exposed to lower effective potentials, counting on CbcBA for channeling electrons out of the cell), or due to a process triggered in response to metabolic needs. On the basis of bacterial counting at +0.4 V and +0.5 V, as addressed in the previous section, we hypothesize that in this case the recruitment of CbcBA at the highest potential would not be attributed to a distance-dependent drop in redox potential throughout the biofilm, but to a metabolic response contributing to the redistribution of energy along the inner membrane by the 're-allocation' of the participation of each of the inner-membrane cytochromes. These findings give way to future studies, e.g. conducted on mutant strains,

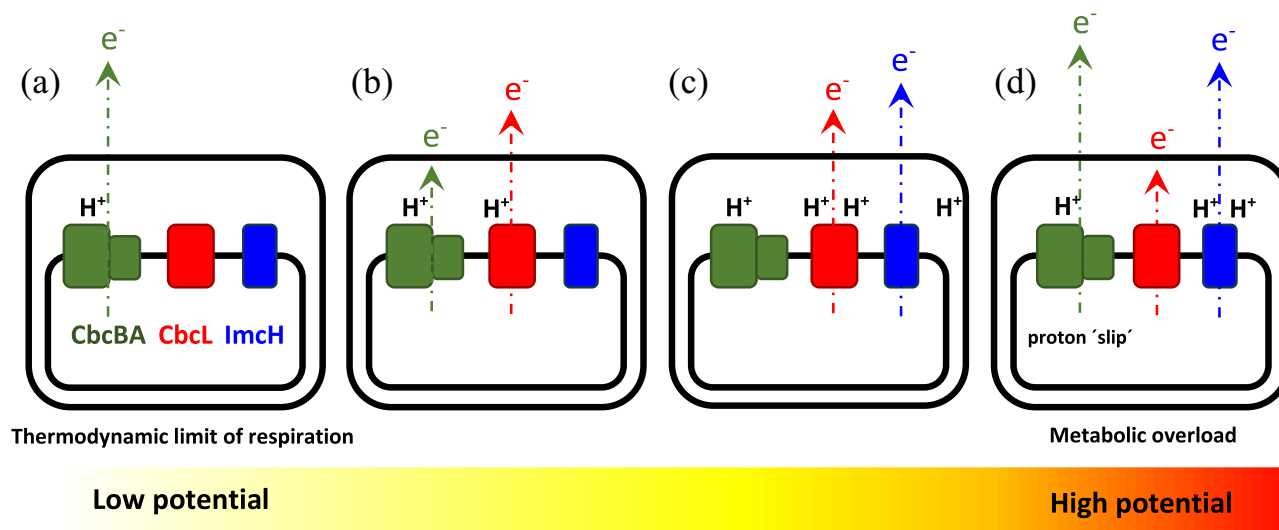


**Fig. 4 | Simplified scheme for the electron-transfer path splitting in *G. sulfurreducens* through CbcBA, CbcL and ImcH as a function of the electrode potential.** The metabolic scenarios corresponding to (a–d) are discussed in the text. The amount of periplasmic protons depicted does not mirror the exact  $H^+/e^-$

stoichiometry, but just emphasizes the building-up of protons as the recruitment of the cytochromes progresses in response to increasing electrode potentials. The basis of the sketch was taken from the representation depicted in the Fig. 1 of ref. 24, so as to expand the interpretation by including the results of the present study.

studies on ATP counting as a function of evolution stage, among others; so as to complement (and eventually support) the proposed hypothesis.

In accordance to our results, we conclude that the CbcBA activity triggered in the biofilm grown at +0.5 V cannot be either attributed to voltammetry scan-induced effects, since, in that case, CbcBA would have been detected in all the stages during growth. Particularly interesting, the overall physiological shifts shown here indicate a certain plasticity in performance of the three inner-membrane cytochromes along the biofilm evolution, with an initial displacement of the catalytic envelope towards higher potentials, then followed by a counteracting shift to lower potentials just before the stationary phase sets in. The dynamic modulation of the inner-membrane behavior suggests a synergistic coupling of the three electron gates over the biofilm evolution, which also gives support to their potential-dependent activities, as depicted in Fig. 1.

#### Revised electron-transfer path model in *G. sulfurreducens*

On the basis of the simultaneous involvement of the three inner-membrane cytochromes in the respiration process, and considering the role of CbcBA as a dissipative path at overloaded respiration, we propose a revised model of the electron-transfer paths in *G. sulfurreducens* as a function of the electrode potential (Fig. 4). The schematic representation, far from establishing a definitive discussion on the topic, is deliberately represented in a simplistic manner, just as a way of expanding the current knowledge on the electron-transfer paths in this microorganism, leaving the door open to new results to come, mainly in the unexplored area of metabolic overloads.

According to its active role as an electron gate near the thermodynamic limit of respiration, CbcBA is used as the main path (with a minor contribution of CbcL) at the lowest potential, consistent with the participation detected for each cytochrome in the biofilms grown at  $-0.23$  V (Fig. 1). This pathway represents a gate that barely conserves energy and that only helps maintaining cell viability supporting microbial life. This scenario is illustrated in the panel (a) of Fig. 4. At higher external potentials, greater transmembrane proton pumping stoichiometries are expected as a consequence of the increasing participation of CbcL to the electron flow, accompanied by the attenuation of CbcBA, as revealed by the inverse relationship observed for both proteins (Fig. 1). This is reinforced when the external potential goes beyond  $-0.1$  V, from which the activity of ImcH becomes increasingly relevant (Fig. 1) leading to higher proton translocation. This is represented in the Fig. 4 by progressively going from panel (b) to (c). This situation leads to an increase of both the *pmf* and the ATP synthesis,

being mirrored in an increasingly higher biomass yield (up to +0.4 V in Fig. 2) and an efficient use of the available catabolic energy at each electrode potential (higher thermodynamic efficiency, Supplementary Material, Section SM-4).

At potentials beyond +0.4 V, the building-up of an excessive transmembrane proton gradient would lead to both the acidification of the periplasm and the maximization of the electrochemical potential, inducing the partial decoupling of the electron-transfer process from the oxidative phosphorylation, this being boosted by either a raise of the electron influx in the respiratory chain and/or a high ATP/ADP ratio. To this respect, two possible decoupling mechanisms have been identified in energy-conserving processes along the inner-membrane of bacteria, also shared by mitochondria during the aerobic ATP synthesis in eukaryotes<sup>40</sup>. One of these mechanisms has been associated to proton gradient degradation - termed 'proton leak' - via decouplers that backflow protons through the plasma membrane (a mechanism coined 'extrinsic uncoupling'). The other mechanism has been related to a decrease of the proton translocation efficiency itself - termed 'proton slip' - via a decreased  $H^+/e^-$  ratio through the use of less thermodynamically-efficient routes with decreased proton pumping stoichiometries ('intrinsic uncoupling'), bypassing the redox hierarchy of the available electron paths<sup>19,40</sup>.

On this background, we propose that intrinsic decoupling mechanisms take part of the electron-transfer process out of *G. sulfurreducens* when the external electrode potential exceeds certain levels (beyond +0.4 V vs SHE). In this scenario, electron paths involving low  $H^+/e^-$  stoichiometries must be used as energy dissipation gates, different from those depending on CbcL and ImcH. According to our results, CbcBA - the only inner-membrane cytochrome in *G. sulfurreducens* demonstrated to barely contribute to the *pmf*<sup>10</sup> - is reactivated at +0.5 V (Fig. 1), becoming a non-energy conserving (dissipative) electron gate when the metabolism is demanded (Fig. 2 and Supplementary Fig. SM-4). The situation of metabolic overload triggering CbcBA activation (at the expense of CbcL attenuation) is represented in the panel (d) of Fig. 4. Regarding the attenuated activity of CbcL at +0.5 V, this fact must have also promoted a concomitant fall in ATP production, thus contributing as well to the overall bacterial biomass drop. In this scenario, alternative mechanisms (yet to be tested) providing additional decoupling routes cannot either be a priori ruled out. As to this, possible partial inhibitions of ImcH and/or porin-cytochromes at extreme potentials - likely inducing the electroactive cells to use different lower- midpotential potential structures - should be also bear in mind, probably complementing the activation of CbcBA.

Once the electrons are transferred through each of the inner-membrane cytochromes, they have to reach out the outer membrane across the periplasm. For this, *G. sulfurreducens* counts on a broad periplasmic electron transfer network, which has been reported to be less responsive to the external potential compared to the inner-membrane cytochromes<sup>41</sup>. This opens up the possibility for CbcBA to loosely interact with a diversity of electron carriers to transport the electrical charge to the outer membrane. Particularly, *G. sulfurreducens* has been demonstrated to make use of a family of five tri-heme redox-mediating periplasmic cytochromes (PpcABCDE) with a variety of characteristics (expression levels, mid-point potentials, Bohr-redox effects), which could take part in the periplasm electron transfer network. Whereas it had been first hypothesized that each Ppc was involved in specific respiratory pathways depending on the external potential and energy needs, they were finally demonstrated to display not only lack of specificity as redox mediators (which would contribute to the respiratory flexibility) but being not completely essential either when an electrode is used as the external acceptor<sup>42</sup>. This supports, on the one hand, the existence of a flexible path bridging the periplasm that might contribute to the electron transfer; and suggests on the other hand that a yet unidentified electron transfer network is employed in *G. sulfurreducens* to channel electrons out of the cell. In this context it is noteworthy that other bacteria, including another model microorganism regarding extracellular reduction of electron acceptors - like *Shewanella oneidensis*<sup>43</sup> - and other Gram-negative bacteria (*Paracoccus denitrificans*)<sup>44</sup> have demonstrated to count on a dynamic periplasmic electron transfer network to impart respiratory flexibility, not sticking to any redox thermodynamic hierarchy, regardless of the growing conditions. This background would give support to the possibility for *G. sulfurreducens* to conduct electrons out of the cell through different pathways bridging the periplasm regardless of the external potential, with CbcBA being activated at high potentials as part of the electron-transfer machinery that provides respiratory flexibility, contributing to prevent the microorganisms from becoming metabolically compromised.

### Concluding remarks

The results of the present study contribute to expanding the current knowledge on energy decoupling mechanisms in bacteria, unveiling the functional activity of CbcBA in *G. sulfurreducens* as a dissipative electron-transfer path triggered when the metabolism is pushed to the limit. In context, this mechanism contributes to impart respiratory flexibility and energy management control, inducing low carbon assimilation when the respiration is forced beyond maximum levels. The recruitment of CbcBA during highly efficient respiratory activities may have relevant practical consequences on the area of bio-electrochemical current generation, counting on just the necessary number of cells to produce maximum amounts of charge per unit time without reaching the stratification limit of the biofilm; at the time that electrode clogging, efficiency losses and stop dead times might be minimized by lowering biomass-to-current ratios.

As electro-activity appears to be widely distributed in the bacterial kingdom, further insights into the regulation of cellular electron flux as a function of the electrode potential - at the level of gene expression - should provide new hints to unveil other or similar mechanisms of energy control in bacteria.

## Methods

### Bacterial strain and planktonic growth conditions

*Geobacter sulfurreducens* (DM12127, DSMZ, Germany) was used as a model electro-active microorganism. Cells were anaerobically grown (80:20 v/v N<sub>2</sub>:CO<sub>2</sub> mixture) in stationary batch at 30 °C, in an aqueous culture medium containing 30 mM KCl, 50 mM NaHCO<sub>3</sub>, 9.3 mM NH<sub>4</sub>Cl, 2.5 mM NaH<sub>2</sub>PO<sub>4</sub>, vitamins and trace minerals, according to previous studies<sup>45</sup>. Prior to inoculation in electrochemical reactors, bacteria were cultured for three weeks in fumarate-containing (40 mM) growth medium (fumarate acting as electron acceptor) supplied with acetate (20 mM) used as the electron/carbon source.

### Growth of *G. sulfurreducens* biofilms

Electro-active *G. sulfurreducens* biofilms were grown in three-electrode electrochemical cells. For this, 5 mL ( $2 \times 10^5$  bacteria/mL) of stationary batch culture medium were inoculated in 150 mL-reactors consisting of a graphite rod (3.5 cm<sup>2</sup> exposed surface area) - used as the working electrode (anode) - a platinum wire (counter-electrode) and a pre-calibrated Ag/AgCl (3 M NaCl) reference electrode. The electrochemical cells, the culture media (continuously stirred) and the feeding reservoirs were all kept at 30 °C under a constant stream of oxygen-free 80:20 N<sub>2</sub>:CO<sub>2</sub> gas mixture to adjust the pH to 7.4. To allow for bacterial growth and proliferation on the anodes, they were polarized at different potentials and the reactors were first left in batch mode for 2 days, after which the systems were turned into a continuous mode. For this, a peristaltic pump was used to inject culture medium (free from electron acceptors and/or planktonic cells) at a flux of 0.12 mL/min. To evaluate the effect of the anode potential on the microbial metabolism, biofilms were separately grown at different external potentials, exploring a potential window spanning the  $-0.23$  V/  $+0.5$  V (vs SHE) range ( $-0.23$  V;  $-0.15$  V;  $0$  V;  $+0.2$  V;  $+0.4$  V and  $+0.5$  V). Polarizations were conducted by using a PGSTAT 101 potentiostat, controlled by the NOVA 1.6 software. The production of current in each case was followed in time by means of chronoamperometric measurements, acquiring 1 point per minute.

### Electrochemical analyses

The anode biofilms grown at different potentials were subjected to catalytic cyclic voltammetry analyses, exploring a  $-0.6$  /  $+0.6$  V potential window (vs the Ag/AgCl reference electrode) at scan rates of 5 mV/s and/or 10 mV/s, for at least three cycles. No voltammetry signal differences were observed for the scan rates tested. The rates used were purposely chosen so as to avoid shifts in electron-transfer path signals (due to cell expression changes) during the voltammetry experiments themselves, according to previous studies<sup>14</sup>. The 10 mV/s scan-voltammogram was used in all cases to evaluate the electron splitting along the inner membrane of *G. sulfurreducens* as a function of the external potential, on the hypothesis of simultaneous multiple electron transfer paths. The contribution of each of the three inner-membrane cytochromes (CbcBA, CbcL and ImcH) to the electron flux out of *G. sulfurreducens* was estimated from a fitting process, according to the approach described by Zacharoff et al.<sup>12</sup> and Howley et al.<sup>14</sup>, based on the expansion of the original model developed by Richter et al.<sup>46</sup>. For the fitting purposes, the anodic scan of the voltammograms was differentiated, and a three-site Nernstian model was employed to reproduce the cumulative current, using midpoint potentials of  $-0.23$  /  $-0.21$  V,  $-0.17$  /  $-0.15$  V and  $-0.07$  /  $-0.05$  V (SHE) for CbcBA, CbcL and ImcH, respectively.

### Microbiological counting procedures

The total number of cells grown on the anodes was determined as a function of the electrode potential. For this, total microbial genomic DNA was isolated from the anode biofilms according to the phenol/chloroform method<sup>47</sup>. Microbial collection was carried out from mature biofilms at the beginning of the stationary phase, so as to avoid physiological stratification events. The extracted DNA was spectrophotometrically quantified ( $\lambda$ : 260 nm), and its purity (absence of proteins) was assessed through the 260/280 nm absorbance ratio. The total number of bacteria was computed from DNA concentrations based on a calibration curve, according to reported protocols<sup>45</sup>. Microbial counting was finally used to determine biomass yields and thermodynamic efficiencies as a function of the external potential.

### Statistics and reproducibility

All the experiments were conducted in duplicate. Potentials at which the electro-active bacteria were grown were selected according to the reported values involving each of the inner-membrane cytochromes, so as to sweep those conditions corresponding to the activation of each metabolic path. Experiments at the different potentials were conducted randomly (not following an increasing (from  $-0.23$  to  $+0.5$  V) or decreasing pattern). Duplicates were performed by following a different order with respect to the first-round experiments, so as to make the assays completely independent

and ensure randomness. Statistical differences in the % of participation of each cytochrome were determined by calculating the mean values and their corresponding standard deviation. To visualize data statistical differences, scatter points corresponding to independent experiments were incorporated in Figs. 1 and 2. No data were excluded from the analyses.

### Reporting summary

Further information on research design is available in the Nature Portfolio Reporting Summary linked to this article.

### Data availability

Source data for the Figures can be found in the Supplementary Data (Excel file). All other data supporting the findings of this study are available within the paper and its Supplementary Information files, or available from the corresponding authors upon reasonable request.

Received: 11 December 2024; Accepted: 24 April 2025;

Published online: 02 May 2025

### References

1. von Bertalanffy, L. The theory of open systems in physics and biology. *Science* **111**, 23–29 (1950).
2. von Stockar, U. Biothermodynamics of live cells: a tool for biotechnology and biochemical engineering. *J. Non Equilib. Thermodyn.* **35**, 415–475 (2010).
3. Barlett, P. N. Bioenergetics and biological electron transport. In: *Bioelectrochemistry: Fundamentals, Experimental Techniques and Applications* (ed. Philip Bartlett) (John Wiley & Sons. Ltd., 2008)
4. Bekker, M., de Vries, S., Ter Beek, A., Hellingwerf, K. J. & Teixeira de Mattos, M. J. Respiration of *Escherichia coli* can be fully uncoupled via the nonelectrogenic terminal cytochrome *bd-II* oxidase. *J. Bacteriol.* **191**, 5510–5517 (2009).
5. Richardson, D. J. Bacterial respiration: a flexible process for a changing environment. *Microbiology* **146**, 551–571 (2000).
6. von Stockar, U. & Liu, J.-S. Does microbial life always feed on negative entropy? Thermodynamic analysis of microbial growth. *Biochim. Biophys. Acta* **1412**, 191–211 (1999).
7. Bond, D. R., Holmes, D. E., Tender, L. M. & Lovley, D. R. Electrode-reducing microorganisms that harvest energy from marine sediments. *Science* **295**, 483–485 (2002).
8. Niebel, B., Leupold, S. & Heinemann, M. An upper limit on Gibbs energy dissipation governs cellular metabolism. *Nat. Metab.* **1**, 125–132 (2019).
9. Zacharoff, L. *Extracellular respiration by Geobacter sulfurreducens: electron pathways are optimized at the inner membrane and substrate interface*, Ph.D. dissertation (University of Minnesota, 2016).
10. Joshi, K., Chan, C. H. & Bond, D. R. *Geobacter sulfurreducens* inner membrane cytochrome CbcBA controls electron transfer and growth yield near the energetic limit of respiration. *Mol. Microbiol.* **116**, 1124–1139 (2021).
11. Pimenta, A. I. et al. Characterization of the inner membrane cytochrome ImcH from *Geobacter* reveals its importance for extracellular electron transfer and energy conservation. *Prot. Sci.* <https://doi.org/10.1002/pro.4796> (2023).
12. Zacharoff, L., Chan, C. H. & Bond, D. R. Reduction of low potential electron acceptors requires the CbcL inner membrane cytochrome of *Geobacter sulfurreducens*. *Bioelectrochemistry* **107**, 7–13 (2016).
13. Levar, C. E., Chan, C. H., Mehta-Kolte, M. G. & Bond, D. R. An inner membrane cytochrome required only for reduction of high redox potential extracellular electron acceptors. *mBio* **5**, e02034 (2014).
14. Howley, E., Krajmalnik-Brown, R. & Torres, C. I. Cytochrome gene expression shifts in *Geobacter sulfurreducens* to maximize energy conservation in response to changes in redox conditions. *Biosens. Bioelectron.* **237**, 115524 (2023).
15. Chan, C. H., Levar, C. E., Zacharoff, L., Badalamenti, J. P. & Bond, D. R. Scarless genome editing and stable inducible expression vectors for *Geobacter sulfurreducens*. *Appl. Environ. Microbiol.* **81**, 7178–7186 (2015).
16. Marsili, E., Rollefson, J. B., Baron, D. B., Hozalski, R. M. & Bond, D. R. Microbial biofilm voltammetry: direct electrochemical characterization of catalytic electrode-attached bacteria. *Appl. Environ. Microbiol.* **74**, 7329–7337 (2008).
17. Verkhovskaya, M. & Bloch, D. A. Energy-converting respiratory complex I: on the way to the molecular mechanism of the proton pump. *Int. J. Biochem. Cell Biol.* **45**, 491–511 (2012).
18. Wikström, M., Krab, K. & Sharma, V. Oxygen activation and energy conservation by cytochrome *c* oxidase. *Chem. Rev.* **118**, 2469–2490 (2018).
19. Wikström, M. & Springett, R. Thermodynamic efficiency, reversibility, and degree of coupling in energy conservation by the mitochondrial respiratory chain. *Commun. Biol.* <https://doi.org/10.1038/s42003-020-01192-w> (2020).
20. Gates, A. J. et al. The relationship between redox enzyme activity and electrochemical potential-cellular and mechanistic implications from protein film electrochemistry. *Phys. Chem. Chem. Phys.* **13**, 7720–7731 (2011).
21. Thauer, R. K., Jungermann, K. & Decker, K. Energy conservation in chemotrophic anaerobic bacteria. *Bacteriol. Rev.* **41**, 100–180 (1977).
22. Rutgers, M., van der Gulden, H. M. L. & van Dam, K. Thermodynamic efficiency of bacterial growth calculated from growth yield of *Pseudomonas oxalaticus* OX1 in the chemostat. *Biochim. Biophys. Acta* **973**, 302–307 (1989).
23. Calhoun, M. W., Oden, K. L., Gennis, R. B., Teixeira de Mattos, M. J. & Neijssel, O. M. Energetic efficiency of *Escherichia coli*: effects of mutations in components of the aerobic respiratory chain. *J. Bacteriol.* **175**, 3020–3025 (1993).
24. Joshi, K., Chan, C. H., Levar, C. E. & Bond, D. R. Single amino acid residues control potential-dependent inactivation of an inner membrane *bc*-cytochrome. *ChemElectroChem*, <https://doi.org/10.1002/celec.202200907> (2022)
25. Calisto, F., Sousa, F. M., Sena, F. V., Refojo, P. N. & Pereira, M. M. Mechanisms of energy transduction by charge translocating membrane proteins. *Chem. Rev.* **121**, 1804–1844 (2021).
26. Wikströma, M. & Hummer, G. Stoichiometry of proton translocation by respiratory complex I and its mechanistic implications. *PNAS* **109**, 4431–4436 (2012).
27. Tran, Q. H. & Uden, G. Changes in the proton potential and the cellular energetics of *Escherichia coli* during growth by aerobic and anaerobic respiration or by fermentation. *Eur. J. Biochem.* **251**, 538–543 (1998).
28. Dietrich, W. & Klimmek, O. The function of methyl-menaquinone-6 and polysulfide reductase membrane anchor (PsrC) in polysulfide respiration of *Wolinella succinogenes*. *Eur. J. Biochem.* **269**, 1086–1095 (2002).
29. Kashket, E. R. Proton motive force in growing *Streptococcus lactis* and *Staphylococcus aureus* cells under aerobic and anaerobic conditions. *J. Bacteriol.* **146**, 369–376 (1981).
30. Blaut, M. & Gottschalk, G. Coupling of ATP synthesis and methane formation from methanol and molecular hydrogen in *Methanosarcina barkeri*. *Eur. J. Biochem.* **141**, 217–222 (1984).
31. Kaila, V. R. I. & Wikström, M. Architecture of bacterial respiratory chains. *Nat. Rev. Microbiol.* **19**, 319–330 (2021).
32. Müller, V. & Hess, V. The minimum biological energy quantum. *Front. Microbiol.* **8**, 2019 (2017).
33. Castro, P. J., Silva, A. F., Marreiros, B. C., Batista, A. P. & Pereira, M. M. Respiratory complex I: a dual relation with H<sup>+</sup> and Na<sup>+</sup>?. *Biochim. Biophys. Acta, Bioenerg.* **1857**, 928–937 (2016).

34. Stuck, J. W. The optimal efficiency and the economic degrees of coupling of oxidative phosphorylation. *Eur. J. Biochem.* **109**, 269–283 (1980).
  35. Howley, E., Ki, D., Krajmalnik-Brown, R. & Torres, C. I. *Geobacter sulfurreducens*' unique metabolism results in cells with a high iron and lipid content. *Microbiol Spectr.* **10**, e0259322 (2022).
  36. Kedem, O. & Caplan, S. R. Degree of coupling and its relation to efficiency of energy conversion. *Trans. Faraday Soc.* **21**, 1897–1911 (1965).
  37. Pietrobon, D. & Caplan, S. R. Use of nonequilibrium thermodynamics in the analysis of transport: general flow-force relationships and the linear domain. *Methods Enzymol.* **171**, 397–444 (1989).
  38. Ishii, S., Watanabe, K., Yabuki, S., Logan, B. E. & Sekiguchi, Y. Comparison of electrode reduction activities of *Geobacter sulfurreducens* and an enriched consortium in an air-cathode microbial fuel cell. *Appl. Environ. Microbiol.* **74**, 7348–7355 (2008).
  39. Schrott, G. D., Ordóñez, M. V., Robuschi, L. & Busalmen, J. P. Physiological stratification in electricity-producing biofilms of *Geobacter sulfurreducens*. *ChemSusChem* **7**, 598–603 (2014).
  40. Kadenbach, B. Intrinsic and extrinsic uncoupling of oxidative phosphorylation. *Biochim. Biophys. Acta* **1604**, 77–94 (2003).
  41. Liu, D.-F. & Li, W.-W. Potential-dependent extracellular electron transfer pathways of exoelectrogens. *Curr. Opin. Chem. Biol.* **59**, 140–146 (2020).
  42. Choi, S., Chan, C. H. & Bond, D. R. Lack of specificity in *Geobacter* periplasmic electron transfer. *J. Bacteriol.* **204**, e00322–e00322 (2022).
  43. Sturm, G. et al. A dynamic periplasmic electron transfer network enables respiratory flexibility beyond a thermodynamic regulatory regime. *ISME J.* **9**, 1802–1811 (2015).
  44. Meschi, F. et al. Efficient electron transfer in a protein network lacking specific interactions. *J. Am. Chem. Soc.* **133**, 16861–16867 (2011).
  45. Massazza, D. A., Parra, R., Busalmen, J. P. & Romeo, H. E. New ceramic electrodes allow reaching the target current density in bioelectrochemical systems. *Energy Environ. Sci.* **8**, 2707–2712 (2015).
  46. Richter, H. et al. Cyclic voltammetry of biofilms of wild type and mutant *Geobacter sulfurreducens* on fuel cell anodes indicates possible roles of OmcB, OmcZ, type IV pili, and protons in extracellular electron transfer. *Energy Environ. Sci.* **2**, 506–516 (2009).
  47. Wilson, K. *Preparation of genomic DNA from bacteria*, *Current Protocols in Molecular Biology (CPMB)* (John Wiley & Sons, Inc., 1997).
- Reviewers of the present study is gratefully acknowledged, which led - throughout the entire reviewing process - to considerable improvements of the discussion of the results.

### Author contributions

D.A.M. and H.E.R. designed the experiments and developed the study. D.A.M., J.P.B. and H.E.R. analyzed the data. H.E.R. prepared the figures. D.A.M., J.P.B. and H.E.R. wrote the manuscript.

### Competing interests

The authors declare no competing interests.

### Additional information

**Supplementary information** The online version contains supplementary material available at <https://doi.org/10.1038/s42003-025-08125-5>.

**Correspondence** and requests for materials should be addressed to Diego A. Massazza or Hernán E. Romeo.

**Peer review information** *Communications Biology* thanks the anonymous reviewers for their contribution to the peer review of this work. Primary Handling Editors: Xiaoling Xu and Joao Valente.

**Reprints and permissions information** is available at <http://www.nature.com/reprints>

**Publisher's note** Springer Nature remains neutral with regard to jurisdictional claims in published maps and institutional affiliations.

**Open Access** This article is licensed under a Creative Commons Attribution-NonCommercial-NoDerivatives 4.0 International License, which permits any non-commercial use, sharing, distribution and reproduction in any medium or format, as long as you give appropriate credit to the original author(s) and the source, provide a link to the Creative Commons licence, and indicate if you modified the licensed material. You do not have permission under this licence to share adapted material derived from this article or parts of it. The images or other third party material in this article are included in the article's Creative Commons licence, unless indicated otherwise in a credit line to the material. If material is not included in the article's Creative Commons licence and your intended use is not permitted by statutory regulation or exceeds the permitted use, you will need to obtain permission directly from the copyright holder. To view a copy of this licence, visit <http://creativecommons.org/licenses/by-nc-nd/4.0/>.

© The Author(s) 2025

### Acknowledgements

This study was financially supported by the National Research Council (CONICET, Argentina) and the National Agency for the Promotion of Science and Technology (ANPCyT, Argentina). The invaluable feedback of the